OPTIMUM BALLISTIC MISSILE TRAJECTORIES AND ASSOCIATED OPTIMUM INTENDED HEIGHT OF BURST OF A WARHEAD

THOMAS J. STILLINGS

OPTIMUM BALLISTIC MISSILE TRAJECTORIES

AND ASSOCIATED OPTIMUM INTENDED

HEIGHT OF BURST OF A WARHEAD

* * * * *

Thomas J. Stillings

OPTIMUM BALLISTIC MISSILE TRAJECTORIES

AND ASSOCIATED OPTIMUM INTENDED

HEIGHT OF BURST OF A WARHEAD

by

Thomas J. Stillings

Lieutenant, United States Navy

Submitted in partial fulfillment of
the requirements for the degree of

MASTER OF SCIENCE
IN
OPERATIONS RESEARCH

United States Naval Postgraduate School
Monterey, California

1 9 6 5

OPTIMUM BALLISTIC MISSILE TRAJECTORIES AND ASSOCIATED OPTIMUM INTENDED HEIGHT OF BURST OF A WARHEAD

by

Thomas J. Stillings

This work is accepted as fulfilling

the thesis requirements for the degree of

MASTER OF SCIENCE

IN

OPERATIONS RESEARCH

from the

United States Naval Postgraduate School

ABSTRACT

A probabilistic model is developed for treating the problem of optimizing the intended trajectory and associated height of burst of a missile-warhead. The angle of re-entry is treated as a control variable. Computational techniques which may be operationally acceptable are described.

TABLE OF CONTENTS

LIST OF ILLUSTRATIONS

I INTRODUCTION

Consider the problem of setting the fusing mechanism of a warhead aboard a ballistic missile in order to optimize the probability of destroying a target.

The general problem as stated above becomes extremely complicated when one considers such things as missile in-flight failures, warhead failures, back-up fusing mechanisms employed, type of warhead and type of burst, distance from launcher to target (which will affect range and Azimuth errors), geodesic error, (i.e., to what degree of accuracy do we know the distance to target.), and more frustrating, the problem of partial kills, i.e., the partial destruction of the target or a portion of the target for a period of time less than the duration of hostilities.

In order to reduce the problem to something that can be handled, it will be convenient to cover briefly three topics: the concept of ballistic coefficient, the reflected (mach) wave phenomenon and the definite range law (cookie cutter).

<u>Ballistic Coefficient</u>:

For our purposes, we may think of the ballistic coefficient as a parameter which describes how much a re-entry vehicle will be affected by the atmosphere (see Fig. 1). It is proportional to the ratio of the weight of the vehicle to its area, i.e., the square of the maximum diameter (see Ref. 4); e.g., for a given area, an increase in weight will tend to

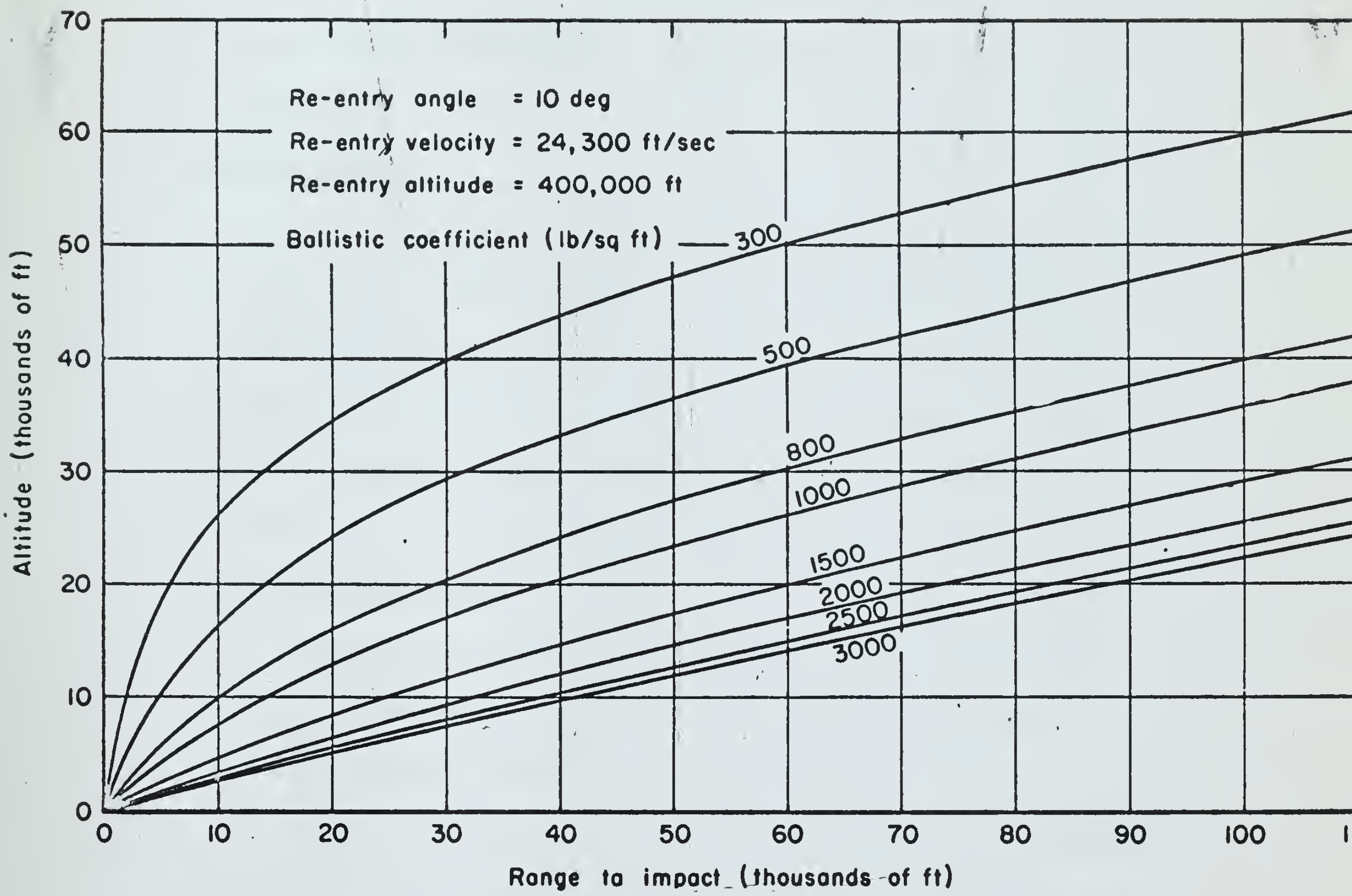

Fig. 1—Trajectory contours for 10-deg re-entry angle

"straighten" the trajectory whereas a decrease in weight will result in a slower re-entry and thereby increase the time spent in the gravitational field. The result will be a more curved trajectory.

Mach Effect:

When a warhead is burst in the air close to ground (e.g., 300 feet for a 1 KT warhead), there is a region of unusually high overpressures due to the merging of the incident and reflected waves (see Ref. 1 and Fig 2). This region is known as the Mach Region. Because of this the curves in Fig. 2 are not monotonic but have the unusual shape exhibited there.

Definite Range Law:

This is the "cookie-cutter" concept that is frequently used. Because of its simplicity it seems to give useful results for many objectives.

A couple of examples should be sufficient for our purposes. Consider a point target in space at which we are firing a projectile with a kill range of one mile. Imagine the target to be at the center of a sphere of radius one mile. If we detonate this weapon anywhere within the sphere we consider the target destroyed; anywhere outside the sphere is considered a miss. Of course, no weapon behaves in such a manner. "Partial kills" are generally the rule rather than the exception, and they are very difficult to quantify. The definite range law is a mathematical convenience. Presumably, this range can be regarded so that a controlled fraction of partial kills will be treated as misses

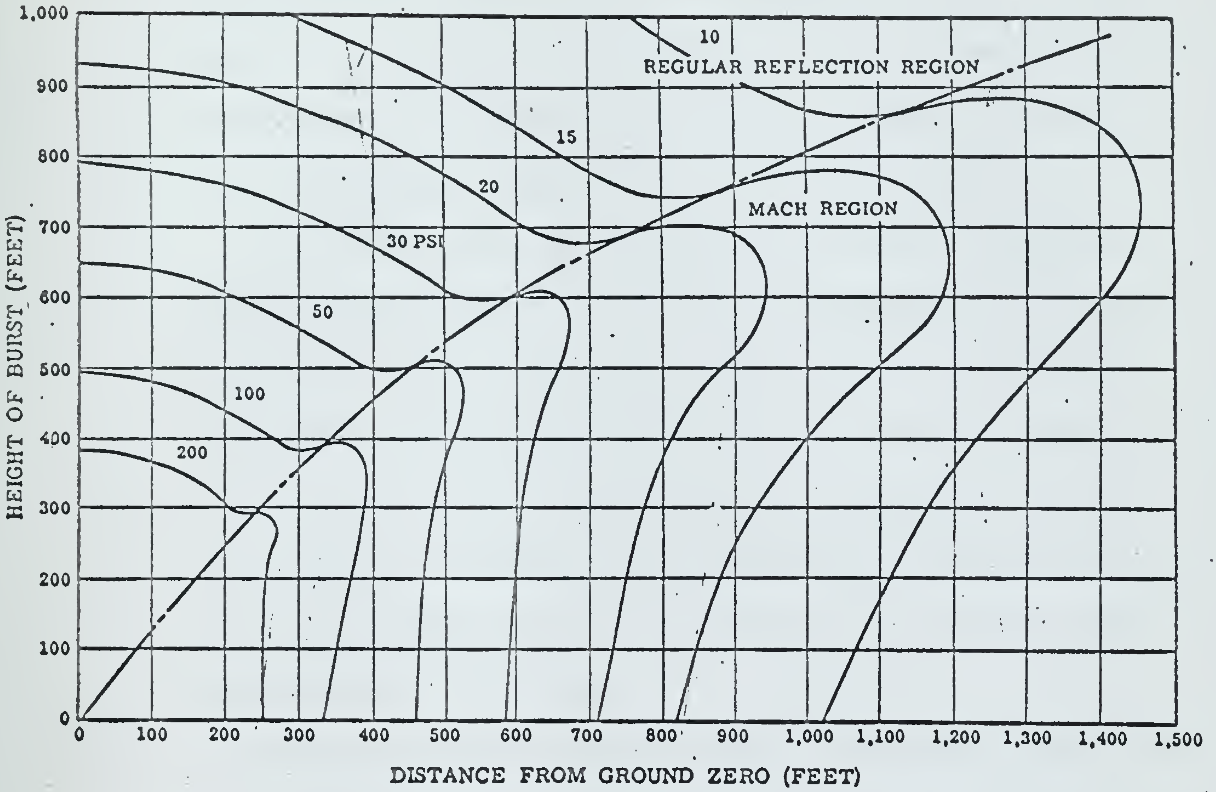

Figure 3.67a. Peak overpressures on the ground for a 1-kiloton burst (high-pressure range).

FIGURE 2

Fig. 2 represents a destruction curve for various overpressures of a 1 KT weapon. For a weapon of different yield W the ordinate and abscissa are each multiplied by $W^{1/3}$. See Ref. 1. For example, a 600 foot high burst of a 1 KT weapon, the 20 P.S.I. curve will extend to about 940 feet from ground zero. Similarly, a 1 MT weapon detonated at 6,000 feet will have a 20 P.S.I. overpressure to about 9,400 feet.

(and a controlled fraction will be scored as hits).

As another example consider Fig. 5. If we imagine a target at (0,0) and estimate that it takes about 20 P.S.I. of overpressure for destruction, the 20 P.S.I. curve shown could be considered as a "cooker-cutter"; i.e., a burst just inside will destroy the target and one just outside will not.

In light of the above discussion, the following three simplifying assumptions will serve as the basis of this paper:

1. The re-entry vehicle has a sufficiently high ballistic coefficient so that the trajectory may be assumed to be a straight line in the neighborhood of the target. Moreover, the vehicle is launched from a sufficiently great distance so that all possible paths may be assumed to be parallel in the neighborhood of the target.
2. The overpressure contours of Ref. 1 (and hence of Fig. 2) are valid and the target damage is a function of overpressure alone.
3. A definite range law holds and 20 P.S.I. is necessary for destruction.

The general objective is to select an optimum height of burst. Further examination of the problem reveals that some other parameters enter into the picture. The angle that the vehicle's trajectory makes with the surface can be selected in advance. There is an advantage to small angles since then the missiles are more difficult to detect (and hence defend against). Larger angles generally lead to higher kill

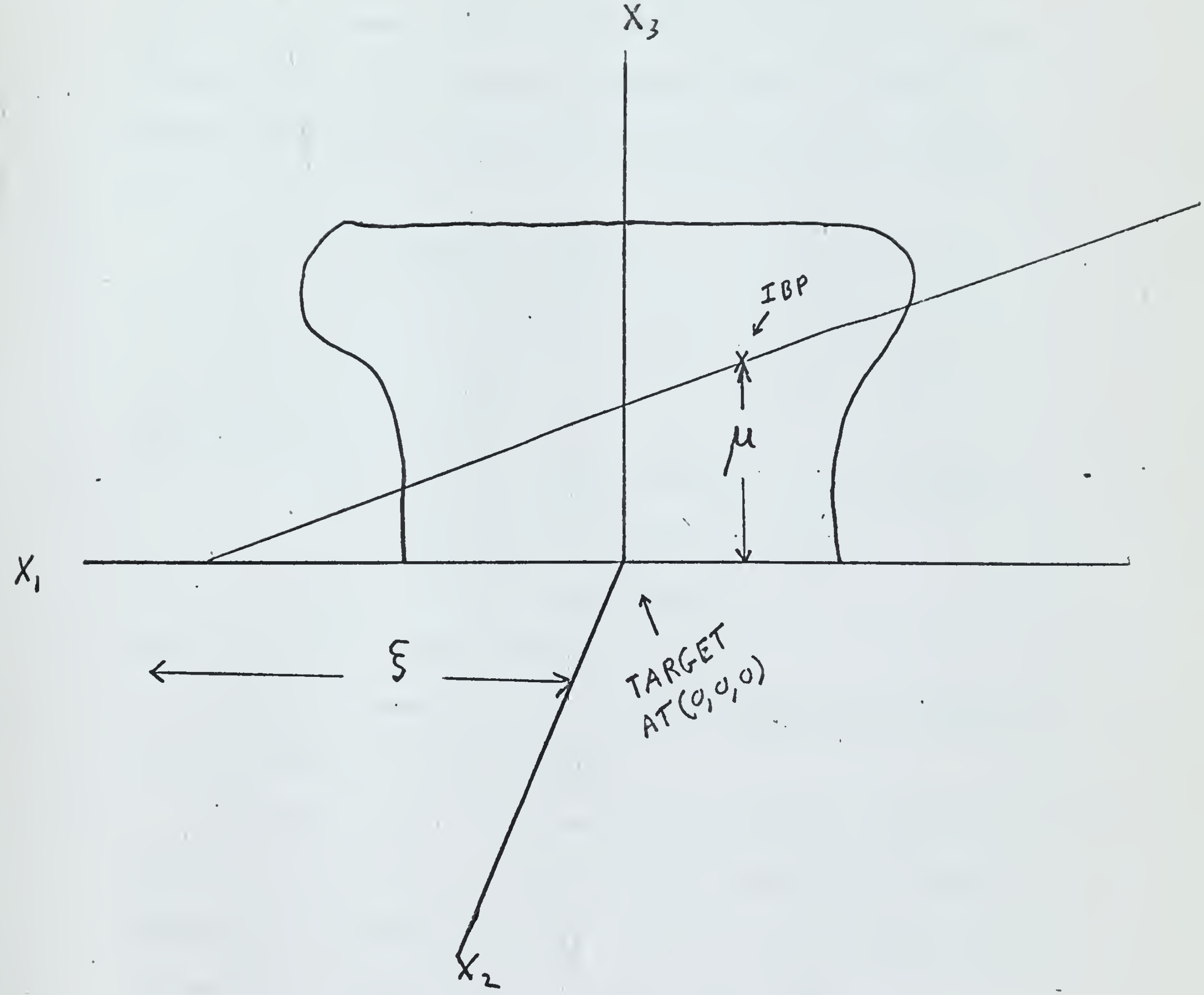

FIGURE 3

DESTRUCTION ENVELOPE

probabilities. The capability to vary this parameter will make defense more difficult. Given a trajectory angle, the optimum burst point becomes a function of height of burst and aim point (intersection of the intended trajectory with the surface). Locating the target at (0,0,0) and using the Cartesian system with

X_1 = downrange distance

X_2 = crossrange distance

X_3 = vertical

and introducing parameters

θ = angle the trajectory makes with the surface

ξ = distance from aim point to target

μ = intended height of burst

(see Fig. 3), the problem now may be stated:

Given θ, choose the pair (ξ , μ) so that the probability of target destruction is maximized.

This paper must be viewed as a pilot study for solving the problem outlined above. It will be noted that a large amount of detailed work remains to be done in order to provide good answers. The methods herein can serve as outlines and guides.

One of the more important results is the development of a graphical computation system using dividers, graphs of over-pressure functions and correction curves. Thus, the optimum solution may be obtained under operational conditions without the need of a digital computer.

The organization of the report is as follows: The mathematical model and nature of the problems of mathematical analysis are presented in section II. The computational problems are described in section III. The operational hand approximations and corrective curves are given in section IV. The conclusions appear in section V. The Monte Carlo technique employed, along with the computer program, appear in Appendices A and B respectively. Appendix C contains a tabulation of the parameter values determined by the graphical method developed in section IV.

II

CONSTRUCTION OF THE PROBABILISTIC MODEL; MATHEMATICAL CHARACTER OF THE PROBLEM

We have already introduced the coordinate system; the angle the trajectory makes with the surface; the intended height of burst μ ; the aim point (ξ , 0, 0). The trajectory is actually a random phenomenon and by assumption 1 can be characterized by the impact point and the incidence angle θ . The actual height of burst is also subject to random errors. Thus, we let

$(Y_1, Y_2, 0)$ be the random vector representing the impact point,

(X_1, X_2, X_3) be the random vector representing the burst point

A sample situation is given in Fig. 4.

It is assumed that:

1. Y_1, Y_2 has a circular normal distribution with mean vector ξ, 0 and covariance matrix $\sigma_1^2 I$ where I is the identity matrix.

2. X_3 has a normal distribution with mean μ, variance σ^2 and is independent of Y_1, and ½.

From Fig. 4 it is seen that $X_1 = Y_1 - X_3 \cot \theta$

$$X_2 = Y_2$$

It follows that the probability density function of the detonation point is

$$f(x_1,x_2,x_3) = \frac{1}{(2\pi)^{3/2}\sigma\sigma_1^2}\, e^{-\frac{1}{2\sigma_1^2}\left[x_2^2+(x_1-\xi+x_3\cot\theta)\right]-\left[\frac{1}{2\sigma^2}(x_3-\mu)^2\right]}$$

The ballistic error parameter σ_1, and the fusing error parameter σ should be determined from independent experiments. There are many types of warheads and fuses and we merely carry σ, and σ_1 as "known" parameters.

Since 20 P.S.I. will destroy the target, the event of target destruction can be visualized in the (X_1, X_2, X_3) space by rotating the curve in Fig. 2 about the vertical axis. If we call this set A, then the probability of target destruction may be expressed as the triple integral of the density function (2.1) over the set A

$$P_D = \iiint_A f(x_1,x_2,x_3)\,dx_1\,dx_2\,dx_3 \tag{2.2}$$

It may be well to clarify a small logical difficulty. The probabilistic model permits negative values for the height of burst. These are physically impossible and should be interpreted as a duded warhead that impacts the surface without exploding.

The optimum solution can be obtained by taking the appropriate partial derivatives of (2.2), equating them to zero and solving the resulting system of equations. Thus

$$\frac{\partial P}{\partial \mu} \propto \iiint_A (x_3-\mu)\, f(x_1,x_2,x_3)\,dx_1\,dx_2\,dx_3$$

(2.3)

$$\frac{\partial P}{\partial \xi} \propto \iiint_A (x_1-\xi+x_3\cot\theta\; f(x_1,x_2,x_3)\,dx_1\,dx_2\,dx_3$$

(2.4) $$\frac{\partial P}{\partial \mu} = 0 \quad , \quad \frac{\partial P}{\partial \xi} = 0$$

Examination of the character of equations (2.4) is facilitated if we make the change of variables

(2.5) $$Y_1 = \frac{X_1 + X_3 \cot \theta}{\sigma_1} \quad , \quad Y_2 = \frac{X_2}{\sigma_1} \quad , \quad Y_3 = \frac{X_3}{\sigma}$$

and let

$$\xi' = \frac{\xi}{\sigma_1} \quad , \quad \mu' = \frac{\mu}{\sigma}$$

In this coordinate system the set A is transformed into a set B the exact nature of which is difficult to visualize (see Fig. 2), but we can say B is bounded since the transformation is linear. In the new system, equations (2.4) may be expressed as

(2.6) $$\left(\frac{1}{2\pi}\right)^{3/2} \iiint_B (Y_3 - \mu) \, e^{-\frac{1}{2}\left[(Y_1 - \xi)^2 + Y_2^2 + (Y_3 - \mu)^2\right]} = 0$$
$$\left(\frac{1}{2\pi}\right)^{3/2} \iiint_B (Y_1 - \xi) \, e^{-\frac{1}{2}\left[(Y_1 - \xi)^2 + Y_2^2 + (Y_3 - \mu)^2\right]} = 0$$

Geometrically, the problem now may be viewed as follows: Given a set B, choose a centering point (ξ, 0, μ) so that the probability of B is maximized.

All solutions of (2.6) are critical points which may be local maxima, minimum or saddle points. The nature of these points may be examined by means of second order derivatives. Letting

(2.7) $$h(Y_1, Y_2, Y_3) = \left(\frac{1}{2\pi}\right)^{3/2} e^{-\frac{1}{2}\left[(Y_1 - \xi')^2 + Y_2^2 + (Y_3 - \xi')^2\right]}$$

we can write

(2.8) $$D_{\mu\mu} = \iiint_B \left[(Y_3 - \mu')^2 - 1\right] h(Y_1, Y_2, Y_3) \, dY_1 \, dY_2 \, dY_3$$

(2.9) $$D_{\mu\xi} = \iiint_B \left[(Y_3 - \mu')(Y_1 - \xi')\right] h(Y_1, Y_2, Y_3) \, dY_1 \, dY_2 \, dY_3$$

(2.10) $$D_{\xi\xi} = \iiint_B \left[(Y_1 - \xi')^2 - 1\right] h(Y_1, Y_2, Y_3) \, dY_1 \, dY_2 \, dY_3$$

A critical point will be a local maximum if

(2.11) $D_{\mu\mu} D_{\xi\xi} - D_{\mu\xi} > 0$ and $D_{\mu\mu} < 0$ (Ref. 3 p. 232)

It can generally be said that $D_{\mu\mu}$ (and $D_{\xi\xi}$, for the same reason) is negative since the variance $\iiint_B (Y_3-\mu')^2 f(Y_1,Y_2,Y_3)\,dY_1\,dY_2\,dY_3$ of Y_3 is one and (2.8) compares a truncated (by B) version of this variance with unity. The remaining part of (2.11) is a difficult question, however, and may require more specific information about the set B.

The set B plays a role in determining the number of critical points. For example, if B were a sufficiently long dumbell shaped region, there would be at least two solutions to (2.6). It would be interesting to examine the question of number of critical points if B were convex. With this condition it may be possible to show there is only one. This contingency was not examined since the set A (and hence B) is not convex.

Since the set A is formed by rotation of Fig. 2 about the X_3 axis, it can be shown that

(2.12) $$\iiint_A x_2 f(x_1, x_2, x_3)\,dx_1\,dx_2\,dx_3 = 0$$

The same must be true in the transformed coordinate system, and it follows from (2.6) and (2.12) that $(\xi, 0, \mu)$ will be the center of gravity of the conditional probability density given (Y_1, Y_2, Y_3) belong to B (if ξ and μ are unique solutions of (2.6)).

III

COMPUTATIONAL PROBLEMS

Computer techniques are required for the solution of the system of equations (2.4), the examination of the critical points (2.11), and the determination of the optimum probability of target destruction (2.2). It was decided to use Monte Carlo techniques (see Appendix A) in this study, and the first step is to characterize the set A. The curve in Fig. 2 may be viewed as giving distance as a function.

This curve is not given in analytic form. Also, note of height, i.e., $g(X_3)$ that there is a small interval of X_3 values for which $g(X_3)$ is double valued. It was decided to ignore the double valued feature and fit a polynomial of order 7 by the method of least squares, using 23 values read directly from the graph. This fit appears in Fig. 8. Using the polynomial as $g(X_3)$, the set A may be represented by

$$(3.1) \qquad A = \left\{ X_1, X_2, X_3 : X_1^2 + X_2^2 \leq g^2(X_3) \right\}$$

The integrals in (2.2), (2.4) and (2.11) all are similar in nature. A rapidly converging iterative technique may generally be available for the solution of the system (2.3).

Letting

$$\phi(x) = \frac{1}{\sqrt{2\pi}} e^{-\frac{1}{2}x^2}$$

the equations (2.4) may be written

$$0 = \iiint_A (X_3 - \mu)\, \phi\left(\frac{X_1 - \xi - X_3 \cot\theta}{\sigma_1}\right) \phi\left(\frac{X_2}{\sigma_1}\right) \phi\left(\frac{X_3 - \mu}{\sigma}\right) dX_1\, dX_2\, dX_3$$

$$0 = \iiint_A (X_1 - \xi + X_3 \cot\theta)\, \phi\left(\frac{X_1 - \xi + X_3 \cot\theta}{\sigma_1}\right) \phi\left(\frac{X_2}{\sigma_1}\right) \phi\left(\frac{X_3 - \mu}{\sigma}\right) dX_1\, dX_2\, dX_3$$

Let functions $g_1(\mu, \xi)$ and $g_2(\mu, \xi)$ be defined so that the above equations are

$$\mu = g_1(\mu, \xi) \quad , \quad \xi = g_2(\mu, \xi)$$

Then, using an initial approximation of μ_0, ξ_0 we can use the iterative scheme

$$(3.3) \quad \mu_{n+1} = g_1(\mu_n, \xi_n) \quad , \quad \xi_{n+1} = g_2(\mu_n, \xi_n)$$

provided it converges.

The examination of the question of convergence usually goes along the following lines: If the series

$$(3.4) \quad \begin{aligned} \mu_n - \mu_0 &= \sum_{j=1}^{n} (\mu_j - \mu_{j-1}) \\ \xi_n - \xi_0 &= \sum_{j=1}^{n} (\xi_j - \xi_{j-1}) \end{aligned}$$

converges absolutely, then μ_n and ξ_n converge to finite numbers which will be the solutions of 2.4. This will take place if a constant r ($0 < r < 1$) can be found such that

$$(3.5) \quad \begin{aligned} |\mu_{j+1} - \mu_j| &\le r(|\mu_j - \mu_{j-1}| + |\xi_j - \xi_{j-1}|) \\ |\xi_{j+1} - \xi_j| &\le r(|\mu_j - \mu_{j-1}| + |\xi_j - \xi_{j-1}|) \end{aligned}$$

for then

$$\sum_{j=0}^{n} |\mu_{j+1} - \mu_j| \le (|\mu_1 - \mu_0| + |\xi_1 - \xi_0|) \sum_{j=0}^{n} j r^j$$

$$\sum_{j=0}^{n} |\xi_{j+1} - \xi_j| \le (|\mu_1 - \mu_0| + |\xi_1 - \xi_0|) \sum_{j=0}^{n} j r^j$$

and

$$\sum_{j=1}^{\infty} j r^j = \frac{r}{(1-r)^2}$$

The question of convergence of the scheme is more easily examined after making the transformation (2.5). Let this be done and write $P_n = \iiint_B \phi(Y_1 - \xi)\phi(Y_2)\phi(Y_3 - \mu)\, dY_1\, dY_1\, dY_3$

and then

$$(3.6) \quad \begin{aligned} g_1(\mu_n, \xi_n) &= \frac{1}{P_n} \iiint_B Y_3 \phi(Y_1 - \xi_n)\phi(Y_2)\phi(Y_3 - \mu_n) \\ g_2(\mu_n, \xi_n) &= \frac{1}{P_n} \iiint_B Y_1 \phi(Y_1 - \xi_n)\phi(Y_2)\phi(Y_3 - \mu_n) \end{aligned}$$

Proceeding as indicated,

$$(3.7)\quad |\mu_{j+1}-\mu_j| \le \left|\frac{1}{P_j}\iiint_B Y_3\phi(Y_1-\xi_n)\phi(Y_2)\phi(Y_3-\mu_j)-Y_3\phi(Y_1-\xi_j)\phi(Y_2)\phi(Y_3-\mu_1)\right|$$

$$+\left|\left(\frac{1}{P_j}-\frac{1}{P_{j-1}}\right)\iiint_B Y_3\phi(Y_1-\xi_j)\phi(Y_2)\phi(Y_3-\mu_1)\right|$$

$$+\left|\frac{1}{P_{j-1}}\iiint_B Y_3\phi(Y_1-\xi_j)\phi(Y_2)\phi(Y_3-\mu_{j-1})-Y_3\phi(Y_1-\xi_{j-1})\phi(Y_2)\phi(Y_3-\xi_{j-1})\right|$$

$$\le \frac{1}{P_j}\iiint_B |Y_3|\phi(Y_1-\xi_j)\phi(Y_2)|\phi(Y_3-\mu_j)-\phi(Y_3-\mu_{j-1})|$$

$$+\left|\frac{1}{P_j}-\frac{1}{P_{j-1}}\right|\iiint_B Y_3\phi(Y_1-\xi_j)\phi(Y_2)\phi(Y_3-\mu_{j-1})$$

$$+\frac{1}{P_{j-1}}\iiint_B |Y_3|\phi(Y_2)\phi(Y_3-\mu_{j-1})|\phi(Y_1-\xi_j)-\phi(Y_1-\xi_{j-1})|$$

From the theorem of the mean

$$\phi(t)-\phi(t') \le |t-t'| \max \phi'(t)$$

it is easily shown that

$$(3.8)\quad |\phi'(t)| \le \frac{1}{\sqrt{2\pi}}e^{-\frac{1}{2}} = \rho < 1$$

and this value may be used in 3.7. Thus we can write

$$|\phi(Y_3-\mu_j)-\phi(Y_3-\mu_{j-1})| \le \rho|\mu_j-\mu_{j-1}|$$

$$|\phi(Y_1-\xi_j)-\phi(Y_1-\xi_{j-1})| \le \rho|\xi_j-\xi_{j-1}|$$

Sharper bounds may be available if the maximum is 3.8 and the points (ξ_j ,0 , μ_j) are constrained to be in the set B. The second term of 3.7 can be estimated in a similar fashion:

$$\left|\frac{1}{P_j}-\frac{1}{P_{j-1}}\right| \le \frac{1}{P_jP_{j-1}}|P_{j-1}-P_j|$$

$$(3.9)\quad \le \frac{1}{P_jP_{j-1}}\left|\iiint_B[\phi(Y_1-\xi_{j-1})\phi(Y_2)\phi(Y_3-\mu_{j-1})-\phi(Y_1-\xi_{j-1})\phi(Y_2)\phi(Y_3-\mu_j)]\right|$$

$$+\frac{1}{P_jP_{j-1}}\left|\iiint_B[\phi(Y_1-\xi_{j-1})\phi(Y_2)\phi(Y_3-\mu_j)-\phi(Y_1-\xi_j)\phi(Y_2)\phi(Y_3-\mu_j)]\right|$$

which can be treated as above.

Collecting, we have

$$
\begin{aligned}
|\mu_{j+1}-\mu_j| \le \; & \frac{1}{P_j}\, \rho\, |\mu_j-\mu_{j-1}| \int_B\!\!\int\!\!\int |Y_3|\, \phi(Y_1-\xi_j)\, \phi(Y_2) \\
& + \frac{1}{P_{j-1}}\, \rho\, |\xi_j-\xi_{j-1}| \int_B\!\!\int\!\!\int (Y_3)\, \phi(Y_2)\, \phi(Y_3-\mu_{j-1}) \\
& + \left\{ \int_B\!\!\int\!\!\int |Y_3|\, \phi(Y_1-\xi_1)\, \phi(Y_2)\, \phi(Y_3-\mu_{j-1}) \right\} \frac{1}{P_j P_{j-1}} \Big\{ \rho\, |\mu_j-\mu_{j-1}| \\
& \int_B\!\!\int\!\!\int \phi(Y_1-\xi_{j-1})\, \phi(Y_2) + \rho\, |\xi_j-\xi_{j-1}| \int_B\!\!\int\!\!\int \phi(Y_2)\, \phi(Y_3-\mu_j) \Big\}
\end{aligned}
\tag{3.10}
$$

which will have the form (3.5) if it can be shown that the coefficients are less than one. This is a difficult analytic problem and is beyond the scope of this paper. The technique (3.3) was used in our computations and lend to answers that were stable in the light of our capability to compute by Monte Carlo. The signs of the determinants (2.11) were computed at the solution values and all were found to be positive.

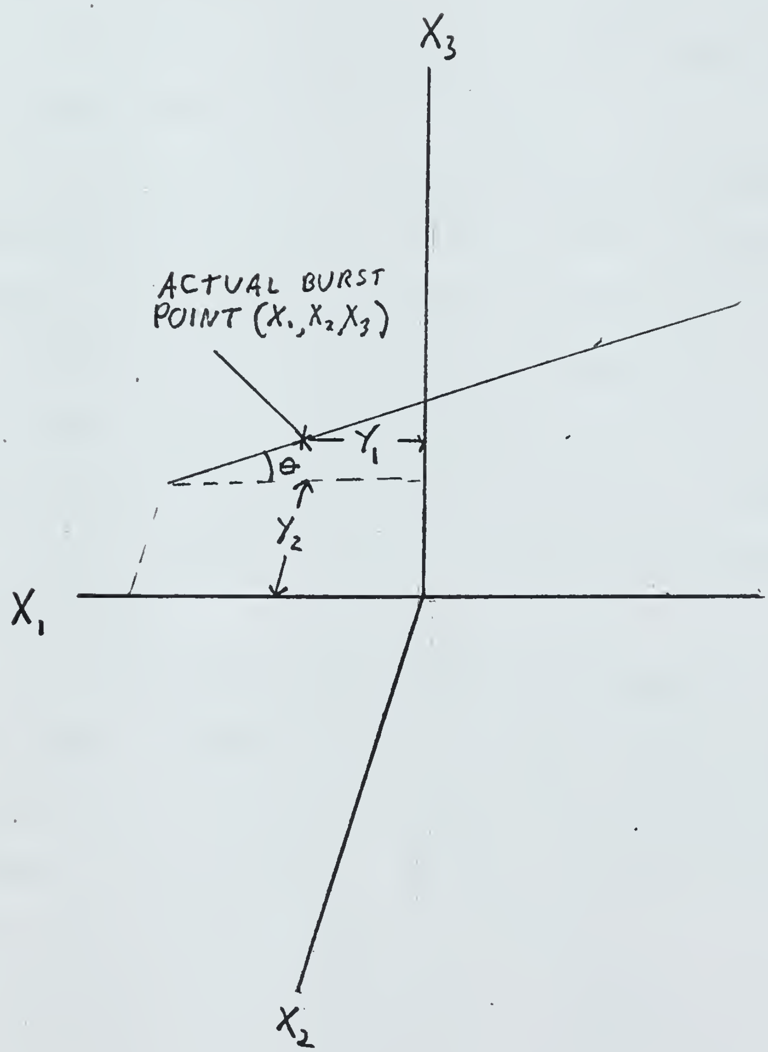

FIGURE 4

SKETCH OF TRAJECTORY AND CO-ORDINATE SYSTEM

IV

A SIMPLIFIED APPROACH TO OBTAIN AN APPROXIMATE SOLUTION; GRAPHICAL METHODS AND CORRECTION

If the down range and cross range errors are assumed to be small, the problem can be reduced to a simple two-dimensional model since we intuitively feel that a 'best' trajectory is one that passes directly over target.

At this point we will assume we follow our intended trajectory with probability 1 and find values of μ and ξ that optimize this conditional probability of destruction.

If Fig. 2 were reflected about a vertical axis, Fig. 5 will result. Again, assume the target to be at (0,0) and we wish to detonate our weapon inside the 20 P.S.I. envelope.

We will make the following assumption to supplement those in section III:

The warhead passes directly over target in a straight line trajectory making an incidence angle of θ with the surface. The collection of possible trajectories will intersect the 20 P.S.I. envelope as shown in Fig. 5. Denote the lower intercept(of a given trajectory) by a and the upper by α.

The maximization takes place in two stages. First, holding θ and ξ fixed, find the best value of μ as a function of ξ. Second, vary ξ until the maximum is obtained. To implement this procedure, let

(4.1) $$F(\mu) = \frac{1}{\sqrt{2\pi}\,\sigma} \int_a^{\alpha} e^{-\frac{1}{2\sigma^2}(Y-\mu)^2}\, dY$$

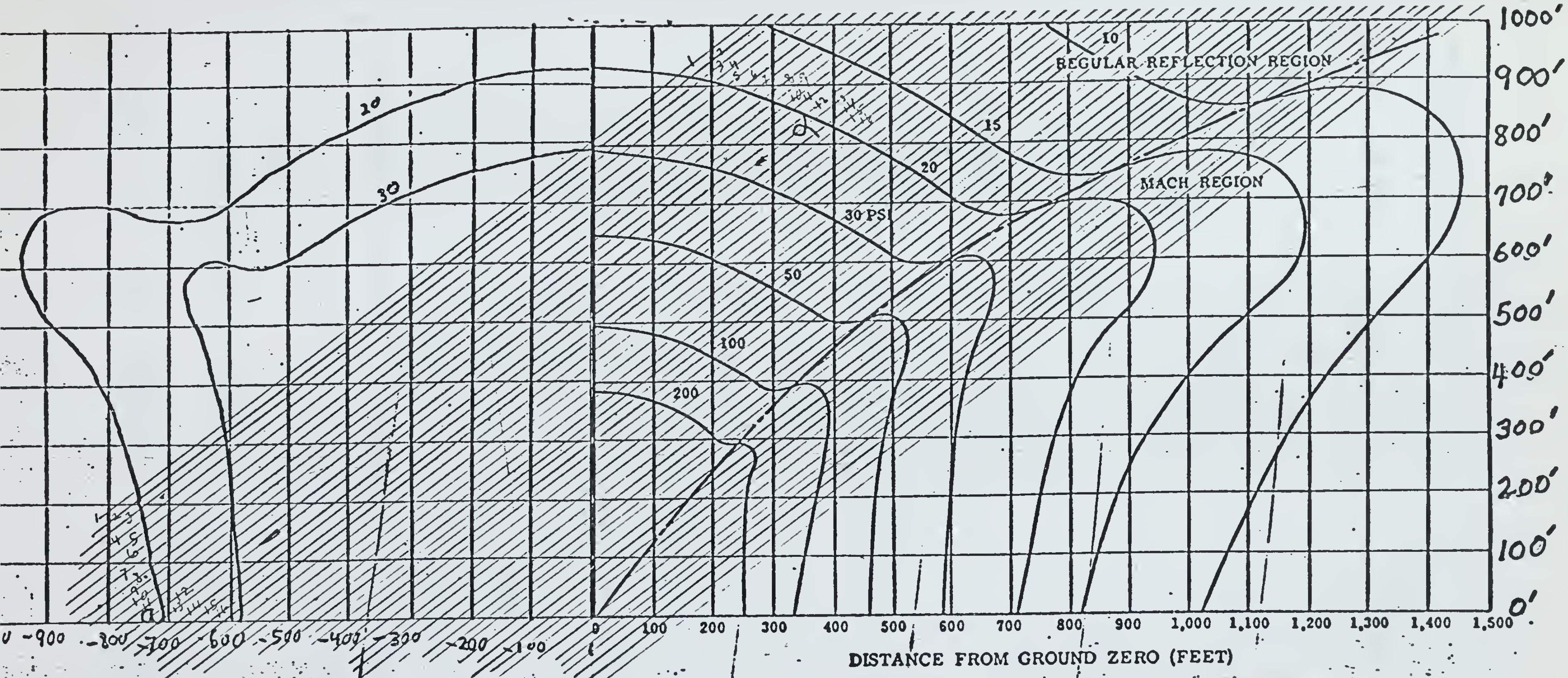

Figure 3.67a. Peak overpressures on the ground for a 1-kiloton burst (high-pressure range).

FIGURE 5

SAMPLE OF METHOD EMPLOYED IN ISOLATING OPTIMUM-INTENDED BURST POINT

Taking the derivative and equating to zero

(4.2) $$F'(\mu) = \int_a^\alpha \frac{1}{\sqrt{2\pi}\,\sigma}\left(\frac{Y-\mu}{\sigma^2}\right) e^{-\frac{(Y-\mu)^2}{2\sigma^2}}\,dY = 0$$

Making the substitution $t = \frac{Y-\mu}{\sigma}$

$$\int_{\frac{a-\mu}{\sigma}}^{\frac{\alpha-\mu}{\sigma}} \frac{1}{\sqrt{2\pi}}\, t\, e^{-\frac{t^2}{2}}\,dt = 0$$

or

$$-\left(e^{-\frac{t^2}{2}}\right)_{\frac{a-\mu}{\sigma}}^{\frac{\alpha-\mu}{\sigma}} = 0$$

$$e^{-\frac{1}{2}\left(\frac{\alpha-\mu}{\sigma}\right)^2} = e^{-\frac{1}{2}\left(\frac{a-\mu}{\sigma}\right)^2}$$

Since a function and its log have a miximum at the same points

$$\left(\frac{\alpha-\mu}{\sigma}\right)^2 = \left(\frac{a-\mu}{\sigma}\right)^2$$

Simplifying and solving for μ

$$\alpha^2 - 2\alpha\mu + \mu^2 = a^2 - 2a\mu + \mu^2$$

$$\mu = \frac{\alpha^2 - a^2}{2(\alpha - a)}$$

(4.3) $$\mu_{MAX} = \frac{\alpha + a}{2} \qquad \alpha > a$$

The problem is degenerate for the case $\alpha = a$ since the probability of detonation is zero. It is interesting to note that the above solution is independent of σ and the velocity of re-entry.

To verify we have a maximum, consider

(4.4) $$F''(\mu) = \int_a^\alpha -\frac{1}{\sqrt{2\pi}\,\sigma}\left(\frac{Y-\mu}{\sigma^2}\right)^2 e^{-\frac{(Y-\mu)^2}{2\sigma^2}}\,dY + \int_a^\alpha \frac{1}{\sqrt{2\pi}\,\sigma}\frac{1}{\sigma^2} e^{-\frac{(Y-\mu)^2}{2\sigma^2}}\,dY$$

Making the substitution $t = \frac{Y - \mu}{\sigma}$ and simplifying we obtain after one integration by parts we see

$$-\frac{(\alpha - a)}{2\sqrt{2\pi}} e^{-\frac{(\alpha - a)^2}{8}} < \frac{\sigma^2}{2}$$

which is true for all $\alpha > a$

The value of F at the point μmax which is the probability of destruction given a particular line is given by

$$F\left(\frac{a+\alpha}{2}\right) = \int_a^\alpha \frac{1}{\sqrt{2\pi}\,\sigma} e^{-\frac{1}{2\sigma^2}\left(Y - \frac{\alpha + a}{2}\right)^2} dY$$

Letting $\tau = \dfrac{Y - \frac{\alpha + a}{2}}{\sigma}$.

$$F\left(\frac{a+\alpha}{2}\right) = \int_{-\frac{\alpha - a}{2\sigma}}^{\frac{\alpha - a}{2\sigma}} \frac{1}{\sqrt{2\pi}} e^{-\frac{\tau^2}{2}} d\tau$$

or

$$\text{(4.5)} \quad F\left(\frac{a+\alpha}{2}\right) = 2\int_{-\infty}^{\frac{\alpha - a}{2\sigma}} \frac{1}{\sqrt{2\pi}} e^{-\frac{\tau^2}{2}} d\tau - 1.0$$

So far we have the optimum height of the IBP, but still must find out where to plan the detonation, i.e., to select ξ . Since we are interested in maximizing the probability of destruction (4.5), we see this is clearly equivalent to maximizing (α -a) since the function is monotonic. Maximizing (α -a) is in turn equivalent to finding the longest line that can be drawn through Fig. 5 at an angle θ .

In Fig. 5, a series of parallel lines were drawn roughly every 20 feet at an angle θ to the horizontal and the longest

line determined by the use of dividers, and choosing the one with max $\{\alpha_i - a_i\}_{i=1}^{n}$. If a maximum occurred between lines it was deemed to be at the mid-point of the two which gives an "accuracy" of 10 feet for a 1 KT weapon or 100 feet for a 1 MT weapon.

By assuming the measurements were accurate in the sense that one can differentiate between a line being longer than an adjacent line (which is reasonable since the vast majority were easily discernable) we can say with probability one, the maximum error is 10 $W^{1/3}$ feet for a W KT weapon.

Measurements were taken in this manner for several values of θ and the resulting values of μmax were plotted against θ. Readings were concentrated at points where the curve appeared to be rapidly changing. A similar procedure was used for values of θ vs X and θ vs $\dot{f}$. in order to interpolate polynomials of degree 1, 2, -----, 20 were fit in a least-squares sense to the data points. The degree chosen from the one with the smallest $\{|Y_i - O_i|\}$ where Y_i = emperical value and 0i = computed value. The above criterion was chosen since it was planned to interpolate values of θ=5, 6, 7, -----, 90 and the measurements were felt to be fairly accurate to start with and large deviations in the fit would only tend to aggrevate the original data points.

The polynomials were fed into the computer and evaluated at the points θ = 5, 6, ----- 90. The results were tabulated

in table 1 where:

μmax = planned burst point measured vertically along HOB axis

XCOORD = planned burst point measured horizontally along "DISTANCE FROM GROUND ZERO" AXIS

θ = Angle trajectory intersects ground measured from the horizontal

ξ = Aim point measured positively to the right along "DISTANCE FROM GROUND ZERO" AXIS

REMARKS CONCERNING THE GRAPHICAL APPROXIMATION

The most interesting discovery is that the 'best' IBP is never over target; for low angles of re-entry, the burst is planned prior to target; for steep angles of re-entry, the IBP is past target.

The sharp discontinuity in XCOORD at about 28° is caused by entry into the envelope in the region (850, 700) of Fig. 5 where the slope of the envelope and the slope of the trajectory are nearly equal.

We will next apply the correction discussed in section III. The method developed above was used as the first approximation for the iterative technique developed in section III. The details follow.

Let $$P = \iiint_{x_1^2+x_2^2 \le g^2(x_3)} \frac{1}{(2\pi)^{3/2}\sigma_1^2\sigma} e^{-\frac{1}{2\sigma_1^2}\left[x_2^2+(x_1-\xi+x_3\cot\theta)^2\right]-\frac{(x_3-\mu)^2}{2\sigma^2}}$$

$$P = \int f$$

$$P_\xi = \int f \frac{1}{\sigma_1^2}(x_1-\xi+x_3\cot\theta) = 0$$

$$P_\mu = \int f \frac{1}{\sigma^2}(x_3-\mu) = 0$$

let $E_1 = \int x_1 f$, $E_3 = \int x_3 f$

$$E_1 - \xi P + \cot\theta\, E_3 = 0$$

$$E_3 - \mu P = 0$$

Solving for μ and ξ

$$\mu = \frac{E_3}{P} , \quad \xi = \frac{E_1 + \mu P \cot\theta}{P}$$

let μ_1, ξ_1 = First approximation obtained by using the method of section IV

$$\mu_n = \frac{E_3}{P} , \quad \xi_n = \frac{E_1 + \mu_n P \cot\theta}{P}$$

In general, about 10 iteratives were needed for $\theta > 10^\circ$ and about 20 for $\theta = 10^\circ$.

Data was collected for $\theta = 10^\circ, 20^\circ$, -----$80^\circ$ for two sets of the standard deviation (σ, σ_1). Table 1 contains the percent of error in μ and ξ and Fig.   contains a plot of θ vs percent of error.

Thus, operational procedures can be developed that do not require a high speed computer. The first approximation is

	$\sigma = 500,\ \sigma_1 = 200$		$\sigma = 200,\ \sigma_1 = 500$	
θ	μ	ξ	μ	ξ
10	+20.8	+0.1	+50	+25
20	+ 7.5	+1.34	+48.9	+71
30	+ 4.28	-1.8	+12.5	+ 5.9
40	+ 7.9	- .134	+ 3.54	-24.2
50	+ 1.5	-4.8	- 6.15	-45
60	+ .065	-2.05	- 5.6	-41.5
70	+ .43	-1.9	- 7.1	-65
80	+ 1.3	-3.2	- 5.8	-14.75

TABLE 1

PERCENT OF ERROR IN μ AND ξ BY USING FIRST APPROXIMATION

$\sigma = 200$
$\sigma_1 = 500$

θ	μ	ξ	PKILL
10	453	2504	.419
20	431	1146	.582
30	432	719	.652
40	440	508	.684
50	438	369	.692
60	438	256	.699
70	435	150	.712
80	438	84	.716

$\sigma = 500$
$\sigma_1 = 200$

θ	μ	ξ	PKILL
10	365	2002	.227
20	315	769	.402
30	391	658	.499
40	459	661	.569
50	472	538	.615
60	468	429	.637
70	463	306	.642
80	471	155	.649

TABLE 2

PROBABILITY OF DESTRUCTION AS A FUNCTION OF RE-ENTRY

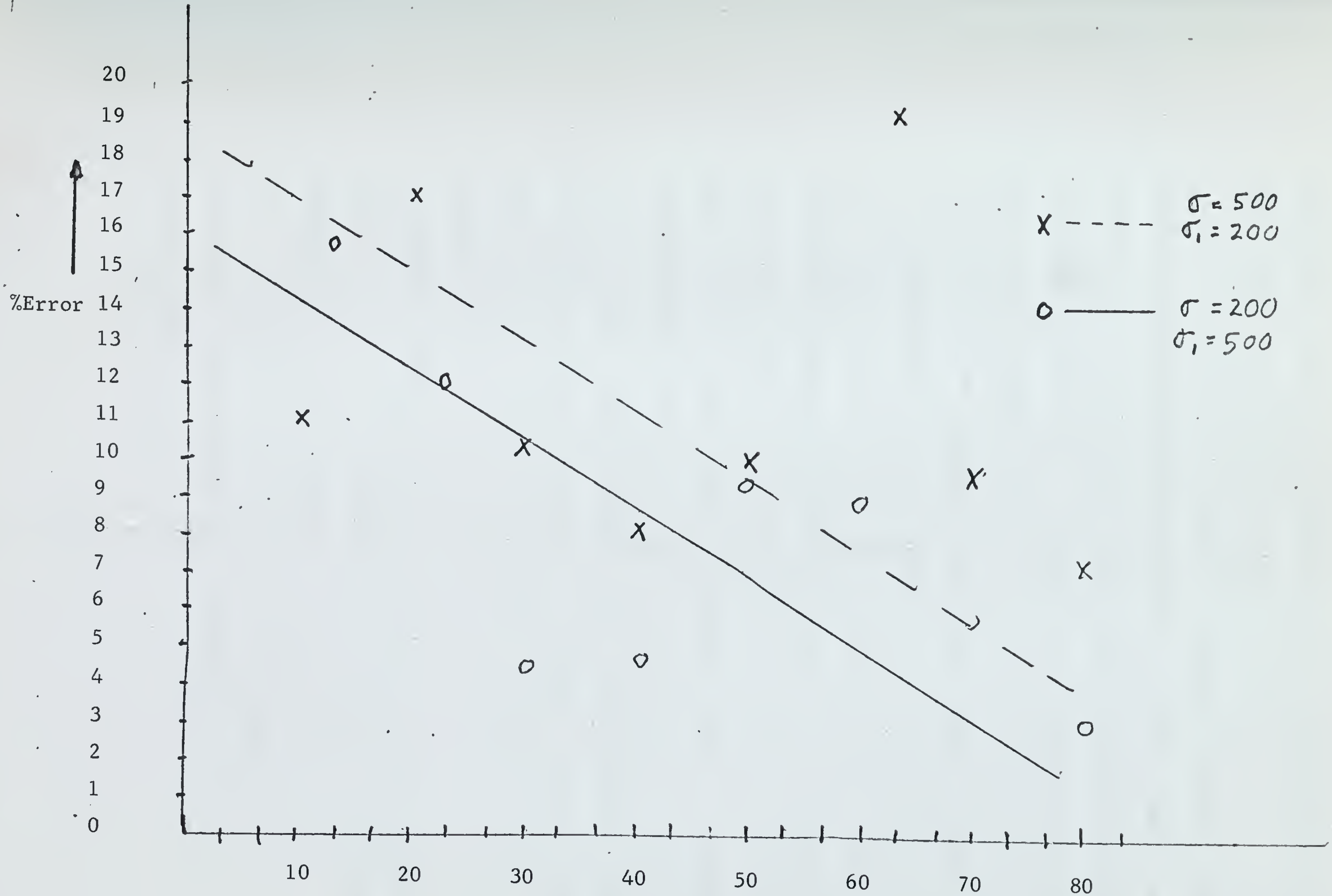

FIGURE 6

GRAPH OF PERCENTAGE ERROR IN PREDICTING PROBABILITY
OF DESTRUCTION VS ANGLE OF RE-ENTRY

obtained by the use of dividers applied to graphs like Fig. 5. The results are corrected by curves like Fig. 6.

As was expected the method of section III gives a more accurate first approximation when the ballistic sigma is small. Probabilities of destruction can be predicted more accurately for higher values of θ. In general, the method of section IV gives values of μ and ξ that are low and nearer to target for small θ ($\theta \leq 40^{\circ}$); high and further from target for higher θ.

This has high intuitive appeal since if re-entry is at a small angle we tend to shoot for the point in Fig. 5 where the destructive envelope intersects the ground. But if ballistic errors are allowed, we run a high risk of having the vehicle impact with the earth before ever reaching target. Similarly, for steep angles of re-entry we tend to aim our errorless vehicle to pass thru the highest point on the envelope since the vertical distance traversed is a maximum. But if we allow errors, we run a high risk of passing to the left of the envelope of Fig. 5.

Appendix C contains a list of starting points (μ_1, ξ_1) for θ = 5, 6, 7, -----, 90 along with associated destruction probabilities. If one chooses to use the curves given in Fig. 5, the destruction probabilities given may serve as a check on the final probabilities, the percent of difference decreasing as σ_1 decreases.

Outside of Appendix C, all probabilities were computed using the polynomial fit to the curve since the curves were not believed to be accurate in the first place and we were interested primarily in technique.

Graphs of the polynomial used and the actual curves are found in Fig. 7.

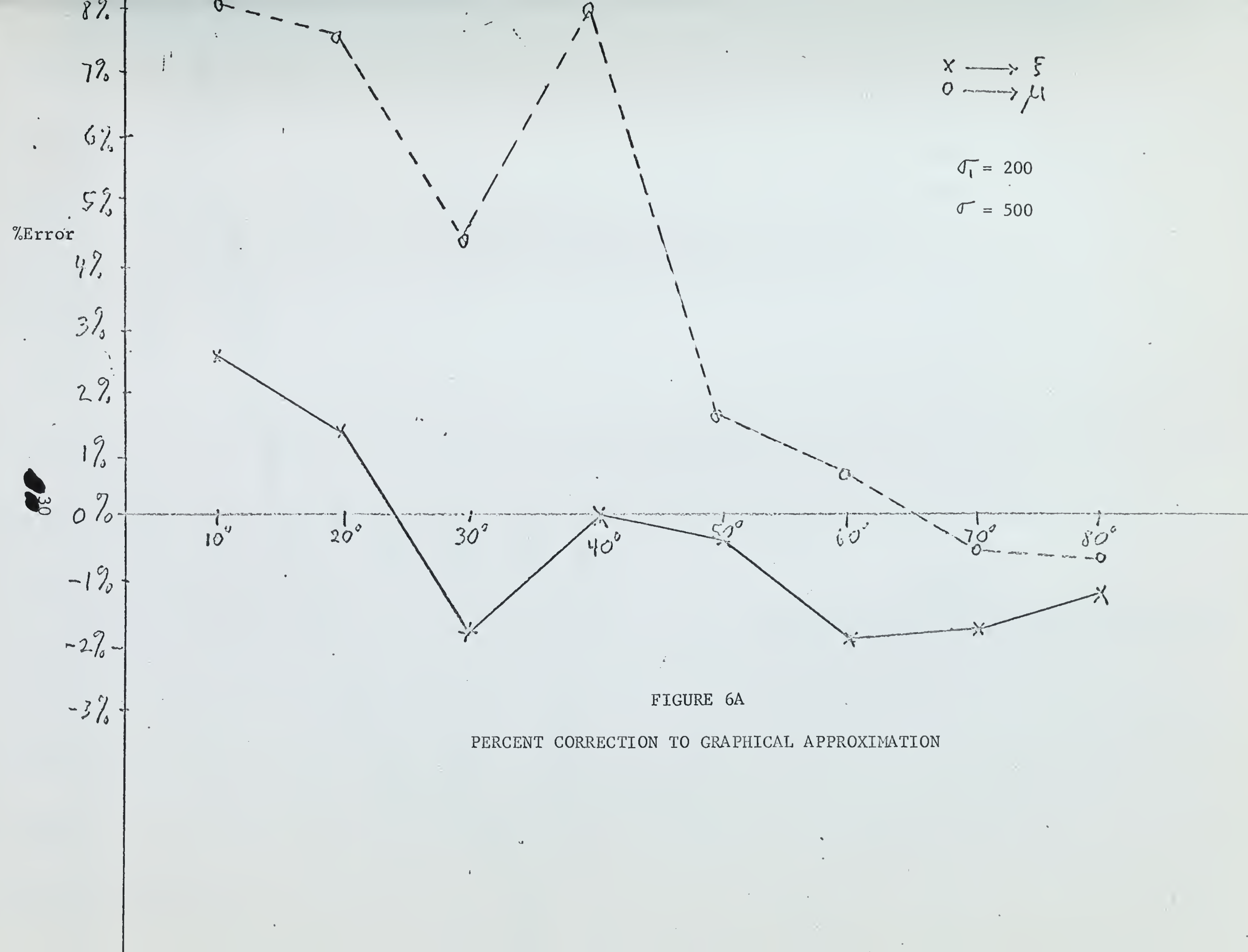

FIGURE 6A

PERCENT CORRECTION TO GRAPHICAL APPROXIMATION

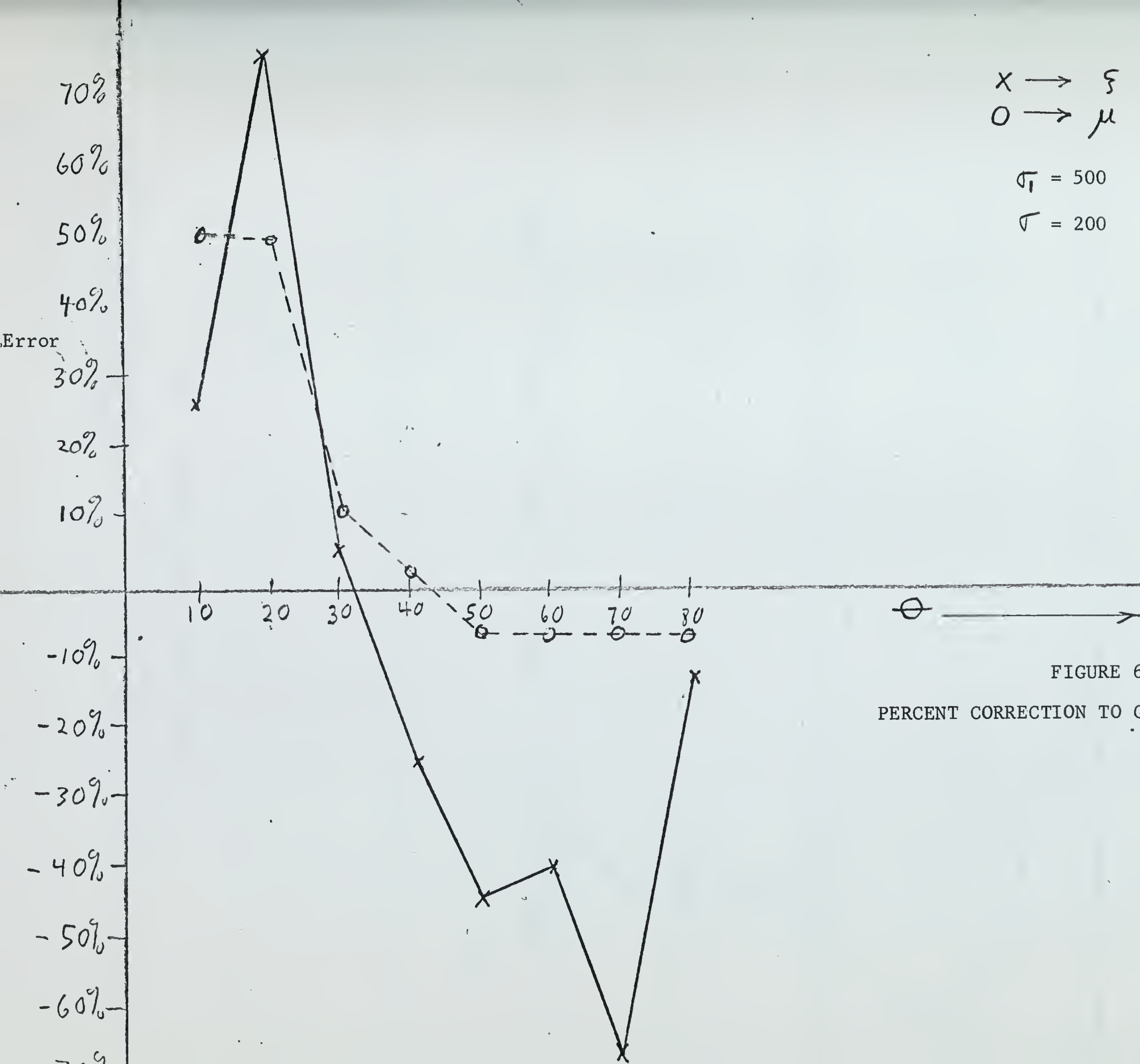

FIGURE 6B

PERCENT CORRECTION TO GRAPHICAL APPROXIMATION

FIGURE 7

PLOT OF ACTUAL DESTRUCT CURVE AND FIT

(both scales in hundreds of feet)

X-SCALE = 2.00E+02 UNITS/INCH.
Y-SCALE = 2.00E+02 UNITS/INCH.

STILLINGS, T.J.
TESTIT

V

CONCLUSIONS

The optimum probabilities of target destruction, and the optimum values of μ and ξ appear as a function of θ in Table 2 for parameter (σ, σ_1) =(200, 500) and (500, 200) ft.

Notice that the fusing error parameter σ is the more important parameter in terms of increasing the probabilities.

This paper should be viewed as a pilot study. The method should be sharpened in the following ways:

1. The overpressure envelope curves (e.g., Fig 2), should be established as a function of yield and mathematical methods of characterizing them (e.g., Fig 7), should be improved.
2. Sharper numerical integration techniques should be applied. The present Monte Carlo method has a 3 standard deviation tolerance of $\pm$ .015 for the probability of destruction.
3. The technique should be applied to a large number of yields using realistic delivery errors and fusing parameters (σ_1 and σ).
4. The hand method for operational computations needs proper development, particularly in the area of sharpening the correction curves (e.g., Fig 6 and Table 1).

For the parameter values used in this study, the probability of destruction was not very sensitive to changes in the values of μ and ξ . This could change with other parameters. For example, a 5 MT weapon delivered from 2000 miles

may well have a delivery error of say σ_1 = 5 miles. If 50 P.S.I. is required for target destruction, it may be necessary to determine μ and ξ very precisely.

It was felt the assumption of a straight line trajectory is fairly realistic and that every moderately large deviation from a straight line will yield approximately the same results since the major dependency is simply in the fusing σ which is largely dependent on the particular warhead and not on the trajectory. Since curved trajectories mean lower speeds, the fusing error σ will be smaller. It follows that the probability of destruction will be higher. Thus, the use of straight line trajectories will yield probabilities which may be used as lower bounds.

The normalicy assumption in the fusing σ is felt to be pretty good if the warhead is fused by a timing mechanism or a radar, but barometric devices are notoriously non-normal.

The circular normal distribution assumed for the trajectory is probably not realistic but is of little consequence since the model is broad enough to include different cross range and down range sigma's if necessary.

The definite range law, as explained in the introduction, generally gives useful results and we feel it is quite appropriate for this problem. It may further be noted that this problem would not be solved were it not for this assumption.

APPENDIX A

A brief description of the integration technique employed.

Again consider a 20 P.S.I. curve in 3-space. We will first enclose the surface in a "box", then choose, at random, a coordinate inside this box. If the coordinate is inside the surface of revolution we record the "height" of the function at that point; otherwise, we record a zero. The sum of these observations divided by the number of observations will give the "average height" of the function over the surface. The average height multiplied by the volume of the box will approximately be equal to the integral of the function concerned. As the number of trials gets large the approximation will, of course, be better.

If we consider each coordinate chosen as a Bernoulli trial, the "worst" the variance could be is $\sigma^2 = \frac{pq}{n}$ where

$p = P_r$ (coordinate is under surface)

$q = 1-p$

$n =$ # of trials

The standard deviation is σ

In our case we chose n = 10,000 which yields an upper bound ($p = q = \frac{1}{2}$) on the deviation as $\sqrt{\frac{1}{4} : \frac{1}{4} : \frac{1}{10{,}000}} = .005$ or a $3\,\sigma$ 'accuracy' of .015

We chose:

Y_1, Y_2 , Y_3= Uniform (0,1) random variables

$X_1 = 2\,c(Y_1 - 0.5)$ $\quad$ X_1 : Uniform (- c, c)

$X_2 = 2\,c(Y_2 - 0.5)$ $\quad$ X_2 : Uniform (- c, c)

$X_3 = b\,Y_3$ $\quad$ X_3 : Uniform (0, b)

(b = 1000, c = 2000 in our case)

If the triple of random numbers (X_1, X_2, X_3) drawn satisfy the inequality $X_1^2 + X_2^2 \leq g^2(X_3)$ the function is evaluated at the point (X_1, X_2, X_3), otherwise a zero is recorded.

Let

$h(X_i)$ = integrand evaluated at (X_1, X_2, X_3) if $X_1^2 + X_2^2 \leq g^2(X_3)$
= 0 otherwise

we know that

$$\lim_{n \to \infty} \frac{1}{n} \sum_{i=0}^{n} h(X_i) \longrightarrow E[h(x)] = \int_{-\infty}^{\infty} h(x)\, p(x)\, dx$$

where $p(X)$ = 1 in our case. The required integral is therefore approximated by

$$b\, c^2\, \frac{1}{n} \sum_{i=0}^{n} h(X_i)$$

USE OF PROGRAM

The following procedure is recommended for finding μ, ξ, and PKILL:

1. Function X GOF must be rewritten to fit destruction curves employed.

2. Values of σ and σ_1 must be changed in the main program to suit the weapon employed.

3. Since only curves for a 1KT weapon are generally available, the problem must first be solved for this case using as a first approximation the value of (μ_1, ξ_1) found by the method of section IV and the parameters μ_1, ξ_1 and σ_1 must be multiplied by $W^{\frac{1}{3}}$ (σ is not a function of the yield since it is inherent in the fusing mechanism).

Conditional probability of destruction given the "best" trajectory when

THETA = angle of re-entry

A = lower intercept of trajectory with destruction envelope

ALPHA = upper intercept of trajectory with destruction envelope

U_{max} = vertical coordinate of IBP

XCOORD = down range horizontal coordinate of IBP

ξ = down range distance from target the trajectory intercepts the ground

APPENDIX B

```
       PROGRAM PROB
      TYPE REAL MU
      DIMENSION MU(50),SI(50)
      PRINT 11
   11 FORMAT(1H1)
      PRINT 14
   14 FORMAT(4X,1HI,5X,5HMU    ,5X,5HSI    ,10HEXPOFX1    ,10HEXPOFX3
     1,10HPKILL     )
      SI(1) = 670. $ MU(1) = 425. $ I = 1
      A=(2.*3.1415926535)**1.5
      B=1./A
  152 THETA = 40./57.2957795131
  153 SIGMA =200.     $ F =SIGMA*SIGMA   $ G=1./F
      CC=TANF(THETA)     $   C = 1./CC
      SIGMA1 = 500.
      D = SIGMA1*SIGMA1
      E = 1./D
      DO 777 LL = 1,70
      N = 0
      VS1 = VS2 = VS3 = 0.
  160 CONTINUE
      Z1 = RANF(-1) $ Z2 = RANF(-2) $ Z3 = RANF(-3)
      X1 = 2000.*(Z1-.5) $ X2 = 2000.*(Z2-.5) $ X3 = 1000.*Z3
      Y1 = X1*X1 $ Y2 = X2*X2 $ Y3 = X3*X3
 1023 W=XGOF(X3)
      WW=W*W
      IF(Y1+Y2.LE.WW) 101,102
  102 V = V1 = V2 = 0.      $ GO TO 575
  101 CONTINUE
      H =SIGMA*D
      P=1./H$Q=B*P
  161 RR = X1-SI(I)+X3*C
      R=RR*RR$S=X2*X2$TT=X3-MU(I)$T=TT*TT
  167 U=EXPF(-.5*((E*(S+R))+T*G))
      V = Q*U $ V1 = X1*V $ V2 = X3*V
  575 CONTINUE
      VS1 = VS1+V $ VS2 = VS2+V1 $  VS3 = VS3+V2
      N = N+1
      IF(N.LT.10000) 160,500
  500  XN=N
      PKILL = 4000000000.*VS1/XN
      E1 = 4000000000.*VS2/XN
      E3 = 4000000000.*VS3/XN
      PRINT 15,I,MU(I),SI(I),E1,E3,PKILL
   15 FORMAT(1X,I4,F10.5,F10.5,F10.5,F10.5,F10.5)
      I = I+1
      MU(I) = E3/PKILL
      SI(I) = (E1+MU(I)*PKILL*C)/PKILL
  777 CONTINUE
      END
```

```
      FUNCTION XGOF (Y)
 1022 B1= 71.1229667E 01
      B2=-31.7485590E-01
      B3= 66.9311997E-03
      B4=-46.2518018E-05
      B5= 14.8951096E-07
      B6=-24.1298172E-10
      B7= 19.0555101E-13
      B8=-58.4969877E-17
      XGOF =  ((((((( B8*Y)+B7)*Y+B6)*Y+B5)*Y+B4)*Y+B3)*Y+B2)*Y+B1
      END
```

APPENDIX C

THETA	A	ALPHA	μ_{max}	XCOORD	ξ
5	499.999	659.945	587	30.023	-64550
6	424.907	660.099	531	60.080	-4899
7	389.185	653.707	505	46.210	-3865
8	369.360	646.386	494	(1.486)	-3178
9	351.793	640.607	487	47.129	-2712
10	329.999	636.991	479	77.037	-2382
11	302.325	635.204	468	90.508	-2131
12	269.999	634.545	454	92.987	-1923
13	235.552	634.304	438	91.381	-1738
14	201.599	633.962	420	91.176	-1564
15	169.999	633.261	401	95.059	-1399
16	141.374	632.210	384	102.720	-1242
17	114.999	631.038	369	111.540	-1096
18	89.067	630.126	356	117.810	-964
19	61.310	629.931	346	118.230	-849
20	29.999	630.912	339	111.320	-753
21	00.000	633.473	334	98.440	-676
22	-00.000	637.916	333	84.139	-620
23	-00.000	644.412	334	75.475	-583
24	-00.000	652.994	336	80.023	-562
25	00.000	663.553	341	102.240	-560
26		675.859	346	137.900	-562
27		689.581	352	166.230	-576
28		704.321	359	139.500	-596
29		719.641	366	-68.566	-620
30		735.102	374	-78.982	-644
31		750.289	381	-90.643	-670
32		764.841	388	-103.780	-687
33		778.468	395	-117.540	-704
34		790.967	402	-131.330	-716
35		802.227	408	-144.830	-725
36		812.226	415	-157.810	-729
37		821.032	421	-170.220	-730
38		828.780	427	-182.160	-728
39		835.665	432	-193.820	-724
40		841.917	437	-205.430	-719
41		847.778	442	-217.220	-714
42		853.488	446	-229.370	-709
43		859.259	450	-241.960	-705
44		865.257	454	-254.920	-702
45		871.596	457	-268.120	-700
46		878.318	460	-281.250	-699
47		885.401	462	-293.940	-700
48		892.748	463	-305.720	-700
49		900.205	465	-316.090	-700
50		907.564	466	-324.550	-700

APPENDIX C (Con't)

THETA	PROBABILITY OF DESTRUCTION SIGMA = 10	50	100	200	500	1000
5	1.000	.890	.576	.311	.127	.064
6		.981	.760	.443	.186	.094
7		.992	.814	.492	.209	.105
8		.994	.834	.511	.218	.110
9		.996	.851	.530	.227	.115
10		.998	.875	.557	.241	.122
11		.999	.904	.595	.261	.132
12		1.000	.932	.638	.285	.145
13			.954	.681	.310	.158
14			.969	.720	.335	.171
15			.979	.753	.357	.183
16			.986	.780	.376	.194
17			.990	.803	.394	.204
18			.993	.824	.412	.213
19			.996	.845	.430	.224
20			.997	.867	.452	.236
21			.999	.889	.477	.250
22			.999	.909	.502	.265
23			1.000	.923	.521	.277
24			1.000	.925	.524	.278
25			.999	.903	.493	.260
26			.999	.909	.501	.265
27			.999	.915	.510	.270
28			1.000	.922	.519	.275
29				.928	.528	.281
30				.934	.538	.287
31				.939	.547	.292
32				.944	.556	.298
33				.948	.564	.303
34				.952	.571	.308
35				.955	.578	.312
363				.958	.583	.315
37				.960	.588	.319
38				.962	.593	.321
39				.963	.5977	.324
40				.965	.600	.326
41				.966	.603	.328
42				.967	.607	.330
43				.968	.610	.323
44				.969	.613	.335
45				.971	.617	.337
46				.972	.620	.339
47				.973	.624	.342
48				.974	.628	.345
49				.976	.632	.347
50				.977	.636	.350

THETA	A	ALPHA	μ_{max}	XCOORD	ξ
51	00.000	909.663	466	-330	695
52		911.767	467	-333	689
53		921.521	467	-334	681
54		930.684	467	-331	669
55		932.232	468	-324	653
56		933.000	468	-315	633
57		933.000	468	-303	611
58			467	-289	585
59			467	-273	556
60			467	-256	526
61			467	-239	496
62			466	-223	466
63			465	-207	438
64			465	-194	412
65			464	-183	389
66			464	-174	371
67			464	-169	356
68			464	-165	345
69			465	-164	338
70			467	-164	333
71			470	-164	330
72			474	-165	326
73			479	-164	322
74			484	-160	314
75			490	-154	301
76			494	-144	283
77			495	-130	259
78			493	-113	230
79			484	-937	196
80			468	-732	160
81			440	-535	126
82			401	-374	986
83			350	-269	801
84			288	-241	756
85			221	-297	865
86			158	-430	111
87			116	-588	142
88			124	-682	161
89			221	-538	136
90			468	-105	165

APPENDIX C (Con't)

THETA		PROBABILITY OF DESTRUCTION					
	SIGMA =	10	50	100	200	500	1000
51		1.000	1.000	1.000	.978	.640	.353
52					.979	.643	.355
53					.979	.646	.357
54					.980	.648	.358
55						.649	.359
56						.649	
57							
58							
59							
60							
61							
62							
63							
64							
65							
66							
67							
68							
69							
70							
71							
72							
73							
74							
75							
76							
77							
78							
79							
80							
81							
82							
83							
84							
85							
86							
87							
88							
89							
90							

BIBLIOGRAPHY

1. "The Effects of Nuclear Weapons", April 1962.

2. Bliss, G. A. Mathematics for Exterior Ballistics. Wiley and Sons, 1944.

3. Meyer, Hebert A. Symposium on Monte Carlo Methods. Wiley and Sons, 1956.

4. Taylor, A. F. Advanced Calculus. Grimm and Co., 1955.